JOURNAL OF Materials CHEMISTRY

Spin density of a ferromagnetic TEMPO derivative: polarized neutron investigation and *ab initio* calculation†

Yves Pontillon,‡[a] André Grand,[b] Takayuki Ishida,[c] Eddy Lelièvre-Berna,[d] Takashi Nogami,[c] Eric Ressouche[a] and Jacques Schweizer*[a]

[a]*Commissariat à l'Energie Atomique, MDN/SPSMS/DRFMC, CEN-Grenoble, 17 rue des Martyrs, 38054 Grenoble Cedex 9, France. Fax: Int code + (33) 4 76 88 51 09; E-mail: jacques.schweizer@cea.fr*
[b]*Commissariat à l'Energie Atomique, SCIB/DRFMC, CEN-Grenoble, 17 rue des Martyrs, 38054 Grenoble Cedex 9, France*
[c]*Department of Applied Physics and Chemistry, University of Electro-Communications, Chofu, Tokyo 182-8585, Japan*
[d]*Institut Laue Langevin, 6 rue J. Horowitz, 156X, 38042 Grenoble Cedex 9, France*

Received 25th January 2000, Accepted 7th April 2000
Published on the Web 13th June 2000

4(*p*-Chlorobenzylideneamino)-2,2,6,6-tetramethylpiperidine-*N*-oxyl is a ferromagnetic TEMPO derivative ($T_c = 0.28$ K) where the nearest and next nearest neighbour NO sites construct a two-dimensional network. We have determined the spin density in this compound by polarized neutron diffraction on a single crystal at low temperature. Most of the spin density (80%) has been found on the NO group, with an equal repartition between the two atoms. 20% of the spin density is delocalized on the rest of the molecule. As for the pure TEMPONE, the two carbon atoms neighbouring the nitrogen of the NO group carry significant spin populations of different signs: −0.074(12) for C3 and +0.069(17) for C4. This implies that the coupling mechanism is rather complex: it concerns many contacts including methyl hydrogens, but also methylene hydrogens, the imino nitrogen N2 and the terminal chlorine atom. *Ab initio* (DFT) calculations account correctly for the repartition of the spin density between nitrogen and oxygen, but they underestimate the part of the spin density which is delocalized and also the effects of the magnetic interactions on the spin populations of adjacent molecules.

Introduction

Looking for ferromagnetism in molecular materials and particularly in purely organic materials is a field of research of growing interest.[1,2] The first genuine organic ferromagnet was found to be the β phase of *p*-nitrophenyl nitronyl aminoxyl with a T_c of 0.6 K[3] while the highest T_c reported in the literature for a purely organic compound is 1.48 K for *N*,*N*′-dioxyl-1,3,5,7-tetramethyl-2,6-diazaadamantane.[4] Recently, several ferromagnetic TEMPO derivatives (TEMPO = 2,2,6,6-tetramethylpiperidine-*N*-oxyl) were discovered with Curie temperatures ranging between $T_c = 0.18$ K and $T_c = 0.4$ K.[5,6] Their behaviour has to be compared to that of pure TEMPONE (4-oxo-2,2,6,6-tetramethylpiperidine-*N*-oxyl), a parent compound, which remains paramagnetic down to 0.05 K.[7] Such a difference has to be connected with the stacking of molecules in the different crystals. In pure TEMPONE, the molecules can be considered as isolated, with shortest distances between the oxygen atoms of the aminoxyl groups of 4.71 Å and 4.94 Å. In all the above ferromagnetic derivatives, the NO sites construct two-dimensional networks and the oxygen atoms are located on zig-zag sheets, the nearest neighbour O···O distances being of the order of 6 Å.[8] These large distances prevent any effect of direct interactions between the N–O sites inside a sheet. However there are interacting methyl and methylene groups which can play the role of ferromagnetic exchange couplers. A mechanism of ferromagnetic interactions inside the sheets has been proposed in references 5 and 9 which implies an alternation of the sign of the spin density when passing from the oxygen atom of one N–O group to the nitrogen atom of the next N–O group *via* a methyl hydrogen, a methyl carbon and a carbon atom of the piperidine ring, as depicted in Fig. 1. The validity of this mechanism was supported by a theoretical calculation, and also by a solid state ^{1}H-MAS-NMR measurement,[10] both of which show negative spin densities on the methyl- and methylene-hydrogen atoms connected to the β-carbons atom of the NO radical site. On the other hand, more detailed ^{1}H and ^{2}D NMR studies and theoretical calculations of another organic-radical ferromagnet, 4-hydroxyimino-TEMPO, clar-

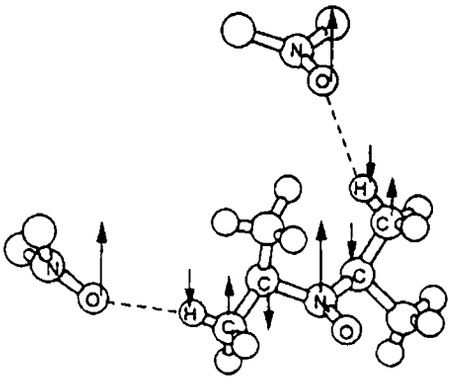

Fig. 1 Mechanism proposed by ref. 5, 9 for ferromagnetic interactions in Cl-TEMPO.

†Positions, isotropic thermal parameters and bond lengths and angles of Cl-TEMPO are available as supplementary data. For direct electronic access see http://www.rsc.org/suppdata/jm/b0/b000691m/
‡*Present address:* Institut Laue Langevin, 6 rue J. Horowitz, 156X, 38042 Grenoble Cedex 9, France.

ified that, whereas all of the β-methylene- and equatorial methyl-hydrogen atoms have negative spin densities, one of the three axial methyl-hydrogen atoms has a positive spin density and the other two methyl-hydrogen atoms have negative spin densities.[11] Rapid rotation of methyl groups results in the averaging of spin densities of the methyl-hydrogen atoms, and, as a result, slightly positive spin densities were observed for axial methyl-hydrogen atoms by NMR. It was postulated that both spin-polarization and hyperconjugation effects must be taken into account for the elucidation of the NMR results.[11]

In order to check this model and to gain some comprehension on the magnetic couplings in this series of TEMPO derivatives, we have investigated by polarized neutron diffraction (PND) the spin density of one of these compounds. We have chosen 4-(*p*-chlorobenzylideneamino)-2,2,6,6-tetramethylpiperidine-*N*-oxyl, of general formula $C_{16}H_{22}ClN_2O$ (to which we shall refer as Cl-TEMPO in the text), a ferromagnetic compound with $T_c = 0.28$ K.[12] The chemical structures of Cl-TEMPO, with its atom labeling used throughout this paper, together with the chemical structure of the parent compounds TEMPONE and TEMPOL, are presented in Fig. 2.

The use of PND to determine the spin density distribution in molecular compounds is now well established.[13,14] It applies to single crystals, generally in their paramagnetic state, in which the magnetization density has been aligned by a strong applied magnetic field. The PND technique (eqn. (1)) consists in measuring the so-called flipping ratios R, of the Bragg reflections, which are the ratio between the diffracted intensities for incident neutron with polarization parallel (+) and antiparallel (−) to the applied magnetic field, respectively:

$$R(K) = \frac{I_+}{I_-} = \left|\frac{F_N(K) + F_M(K)}{F_N(K) - F_M(K)}\right|^2 \quad (1)$$

In the case of centric structures, these flipping ratios yield the value of the ratio between the magnetic structure factor, (F_M), and nuclear structure factor (F_N). Consequently, the experimental F_M values can be deduced considering the nuclear structure factors determined from the unpolarized neutron diffraction experiment. The spin density map can then be reconstructed from these F_M values.

We describe the experimental aspect of this work in the next section. In the third section we examine the crystal structure, refined at low temperature from the unpolarized neutron experiment. Then we explain briefly how the polarized neutron data have been treated to give a spin density map, and we compare the experimental results to those obtained by density functional theory (DFT) calculations. Finally, we discuss the possible magnetic couplings in this compound.

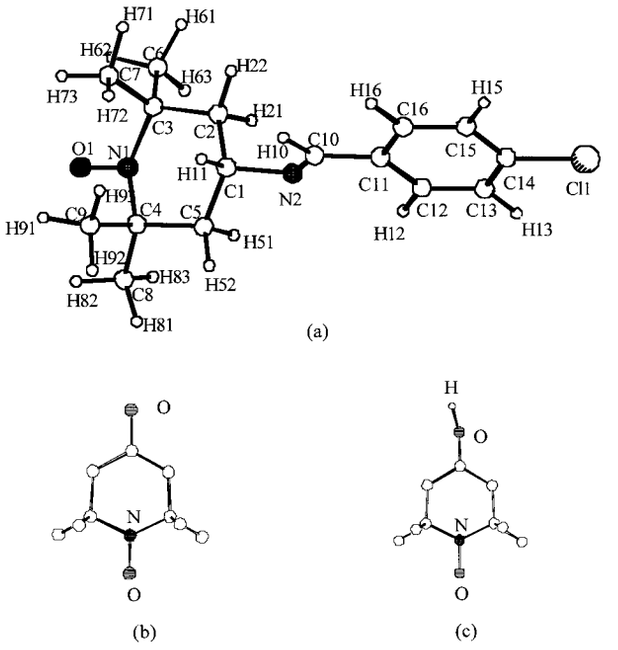

Fig. 2 Chemical structures (a) of the Cl-TEMPO molecule, and of the parent compounds: (b) TEMPONE and (c) TEMPOL.

Experimental

Spin densities are measured by polarized neutron diffraction. These experiments are generally conducted at liquid helium temperature or below, and, as explained above, it is necessary to know exactly the positions and the thermal parameters of all the atoms of the compound at this low temperature. As the crystal structure of Cl-TEMPO has been determined by X-ray diffraction, at room temperature,[8] only the "heavy" atoms (all the atoms except the hydrogens) were located, and their position and vibration parameters were known at room temperature only. We have then performed another diffraction experiment, at low temperature, with unpolarized neutrons, in order to "locate" all the atoms, including the hydrogen atoms and to get a good knowledge of the crystal structure in the same conditions as those in which the spin density has been investigated.

The crystal structure experiment was performed on the unpolarized neutron diffractometer D15 of the Institut Laue Langevin, Grenoble, at a wavelength $\lambda = 1.173$ Å. This diffractometer has a lifting counter and can accommodate a liquid helium cryostat in which the samples were cooled down to $T = 4.5$ K. Two crystals have been used: crystal **1** of dimensions $6 \times 2 \times 2$ mm^3, mounted with the ***a*** axis vertical, allowed to collect the integrated intensities of reflections such as 0*kl*, 1*kl*, 2*kl*... Crystal **2**, of dimensions $3.5 \times 2.5 \times 1$ mm^3, was mounted with axis ***b*** vertical,[15] in order to collect reflections of type *h*0*l*, *h*1*l*, *h*2*l*...

The spin density experiment was performed on the polarized neutron diffractometer D3 of the ILL, Grenoble, at a wavelength $\lambda = 0.843$ Å. This instrument is also a lifting counter diffractometer, with a cryomagnet which holds the sample and provides a vertical magnetic field of 4.5 T. We have mounted crystal **1** on D3, with the ***a*** axis vertical and parallel to the applied field. We have measured the flipping ratios of 246 independent reflections up to $\sin\theta/\lambda = 0.50$ Å^{-1}. During the experiment, the temperature of the crystal was kept at $T = 1.5$ K.

Finally, as the magnetization induced by the applied field corresponds to the magnetic structure factor $F_M(000)$, magnetic investigation of Cl-TEMPO powder was done on a commercial Quantum Design SQUID magnetometer in the same conditions as for the polarized neutron experiment ($T = 1.5$ K and $H = 4.5$ T). A value of $M = 0.985\mu_B$/molecule was obtained.

Crystal structure refinement§

Cl-TEMPO crystallizes in the monoclinic space group $P2_1/c$. The lattice constants, as determined at room temperature by X-rays and at $T = 4.5$ K by neutrons are reported in Table 1, together with the relevant crystal refinement data.

The integrated intensities have been corrected for absorption ($\mu = 2.34$ cm^{-1}). The position parameters and the anisotropic thermal parameters B_{ij} of all the atoms were refined at low temperature using the program ORXFLS.[16] Extinction turned out to be significant. It was modeled in the approximation of the Gaussian mosaic crystal with scattered intensities corre-

§CCDC reference number 1145/221. See http://www.rsc.org/suppdata//jm/b0/b000691m/ for crystallographic files in .cif format.

Table 1 Lattice constants determined at $T=298$ K by X-rays and $T=4.5$ K by neutrons and relevant parameters of the crystal refinement

T/K	4.5	298
a/Å	5.736 (9)	5.909
b/Å	23.946 (11)	24.475
c/Å	11.322 (10)	11.421
β/°	104.36 (9)	103.84
M/g mol^{-1}	293.5	
Cryst. system	Monoclinic	
Space group	$P2_1/c$	
Z	4	
μ/cm^{-1}	2.34	
No. refl. meas.	(1) 1944 (2) 1135	
No. refl. ind.	(1) 1209 (2) 897	
$wR(F^2)$	0.055	

sponding to a secondary extinction of type II.[17] The refinement went quite well with $wR(F^2)=5.50$, $\chi^2=1.51$.

The structure of the compound is displayed in Fig. 3a, 3b and 4. The positions x, y, z and the isotropic thermal parameters B_{eq} at low temperature are available as supplementary materials (Table S1). A comparison of the bond lengths and the bond angles at $T=298$ K and $T=4.5$ K is given in Tables S2, S3a and S3b, a full list of the anisotropic vibration

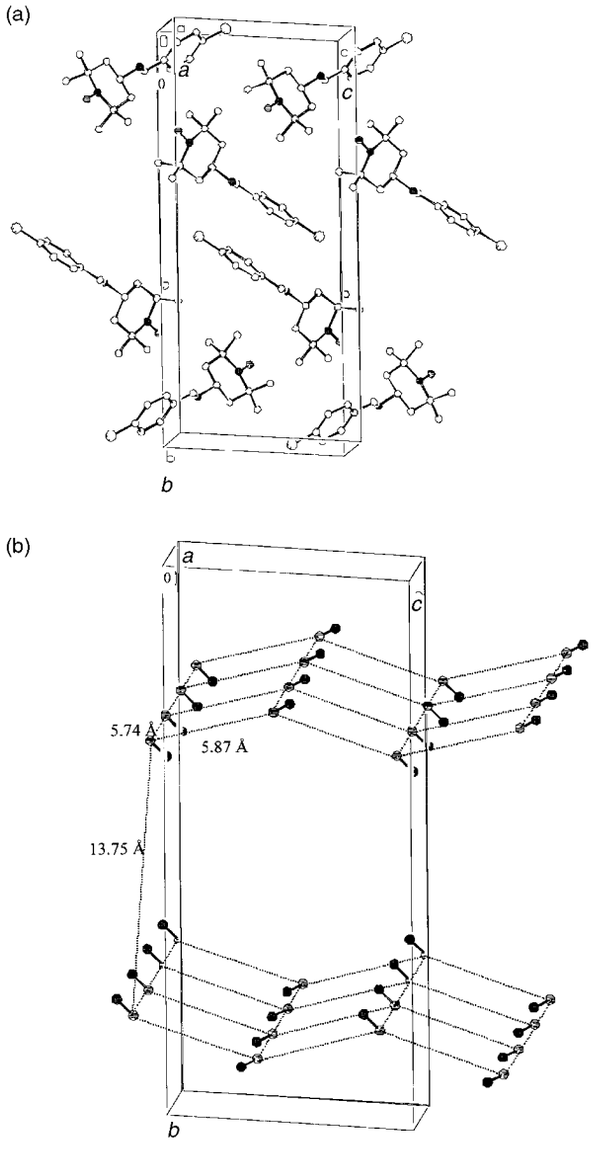

Fig. 3 Crystal structure of the Cl-TEMPO: (a) Crystal packing (b) Zig-zag sheets of the NO groups.

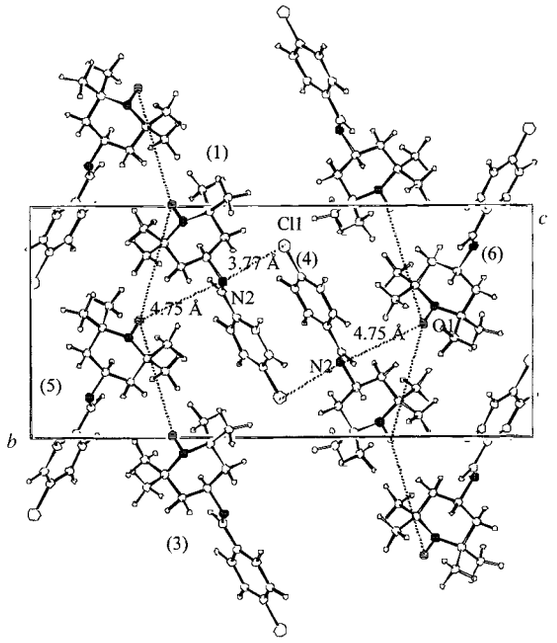

Fig. 4 Crystal structure of Cl-TEMPO projected along the ***a*** axis of the unit cell.

parameters B_{ij} at $T=4.5$ K in Table S4 and all the details of the refinement in Table S5 (supplementary materials).†

On the whole the distances and bond angles inside the molecule have changed very little when cooling from room to low temperature. The distances and angles which have changed are those which connect atoms belonging to different molecules.

As shown in Fig. 3b, the NO sites construct two-dimensional networks and the oxygen atoms are located on zig-zag sheets, parallel to the (***a***,***c***) plane. The nearest neighbour O···O distances which were 5.91 Å and 5.95 Å at room temperature are now 5.74 Å and 5.87 Å at low temperature. During cooling, the intersheet O···O distance (roughly along ***b***) grows from 10.86 Å to 13.26 Å. Linking two sheets, the aryl groups are face to face and inverted, the distance between two aryl groups being $\approx$4 Å (Fig. 3a).

Inside the zig-zag sheets, contacts exist between molecules along the ***a*** direction. These contacts connect atom O1 from molecule 1 to methyl atoms H72 and H93 of molecule 2 at distances 2.62 Å and 2.49 Å respectively. Other O···H contacts are at larger distances (Fig. 5a).

In the same zig-zag sheet, along the ***c*** direction, contacts connect atom O1 from molecule 5 to methyl atoms H61 and H63 of molecule 1 at distances 2.37 Å and 3.40 Å respectively. One has to note also the existence between these two molecules of a contact between O1 of molecule 5 and methylene hydrogen atom H22 of molecule 1 at a distance of 2.73 Å (Fig. 5b). The distance between the O1 atom of molecule 5 and the imino nitrogen N2 of molecule 1 is only 4.75 Å (Fig. 4).

Along the ***b*** axis a contact exists between the terminal Cl of molecule 1 and the imino nitrogen N2 of molecule 4 at a distance of 3.77 Å (Fig. 4).

Experimental spin density determination

The different ways to analyze the polarized neutron data in order to get spin density maps from the magnetic structure factors[18] have already been explained.[19,20,21] Here, we have used two of them: the maximum of entropy (MaxEnt) which permits the reconstruction of the density distribution without any assumption on its nature and the orbital modeling method, which corresponds to a parameterization of the spin density.

Fig. 6 and 7 show the projections parallel to z and y of the

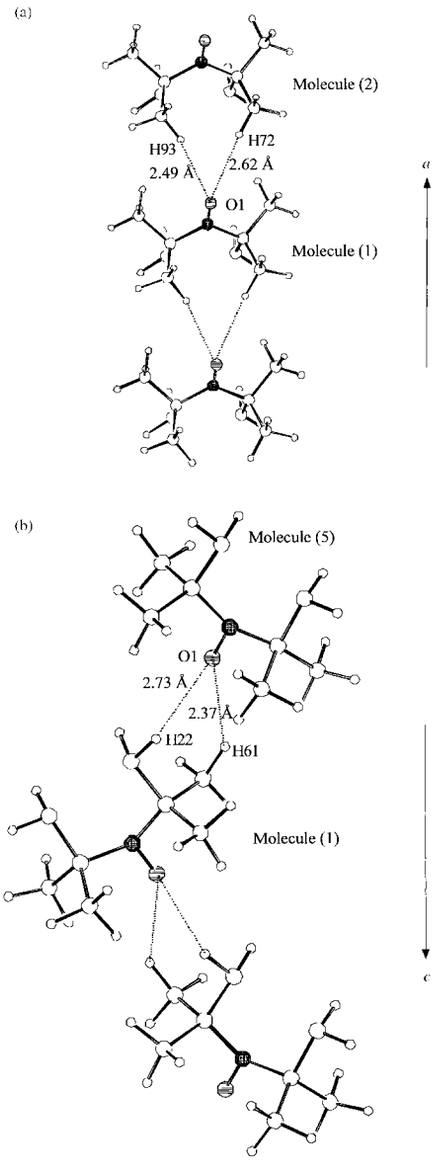

Fig. 5 Intermolecular contacts (a) between the NO group of molecule 1 and the hydrogen atoms of molecule 2, (b) between the NO group of molecule 5 and the hydrogen atoms of molecule 3.

MaxEnt distribution, respectively (axis x is along O1–N1, axis y nearly parallel to C3–C4, axis z is perpendicular to the other two). These projections indicate that most of the spin density is carried by the nitrogen and the oxygen atoms of the aminoxyl group and that the amount of spin density on these two atoms is nearly equal. Furthermore, the shape of the projections clearly shows that the spin density corresponds to 2p orbitals on the N and the O atoms. A careful examination of Fig. 7 brings two more pieces of information. First, the center of gravity of the density on the nitrogen atom does not coincide with the position of atom N1 but is slightly removed away from the center of the N1–O1 bond, which can be interpreted as a signature of the antibonding character of the molecular orbital. Second, the atomic 2p orbitals, both on O1 and N1 are slightly rotated in the π plane, from the z direction. This point will be reexamined later. Furthermore, MaxEnt method fails to reconstruct the small spin density which exists on the atoms of the carbon skeleton. This weakness of the method is well known,[22] and another method will be used to reveal the weaker part of the spin density.

For the orbital modeling, the parameters for all the carbon, chlorine, nitrogen and oxygen atoms of the molecule as well as the methyl and methylene hydrogen atoms of the piperidine

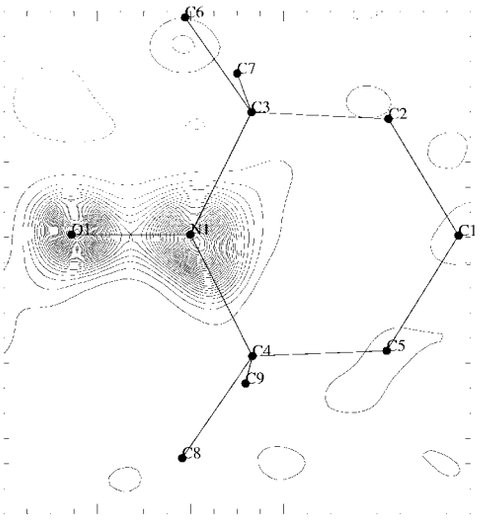

Fig. 6 Spin density reconstructed by MaxEnt and projected along the z-axis (contour step: 0.025 μ_B Å^{-2}).

ring were refined. On the nitrogen and the oxygen atoms of the aminoxyl group, the magnetic orbital was expanded in functions of $|2p_x\rangle$, $|2p_y\rangle$, and $|2p_z\rangle$. The radial exponents ζ, which are tabulated as $\zeta_N = 1.95$ and $\zeta_O = 2.25$ atomic units for nitrogen and oxygen in the literature,[23] were refined to $\zeta_N = 2.36(9)$ and $\zeta_O = 2.40(9)$. The local axes of these atoms are the same as in the former paragraph. The contributions of the other atoms were approximated by a spherical density, and their radial exponents ζ were taken in the same reference:[23] 1.72, 2.20 and 1.25 atomic units for carbon, chlorine and hydrogen atoms respectively.

Table 2 displays the refined individual atomic populations S_i. Fig. 8 and Fig. 9 represent the high and low contours of the spin density reconstructed by this method and projected along the local z axis of site N1. As seen by MaxEnt, most of the density is concentrated on the aminoxyl group. The contribution of these atoms to the magnetic molecular orbital are given by eqn. (2) and (3):

$$\psi_M^O = 0.164(111)|2p_x\rangle - 0.100(68)|2p_y\rangle + 0.981(6)|2p_z\rangle \quad (2)$$

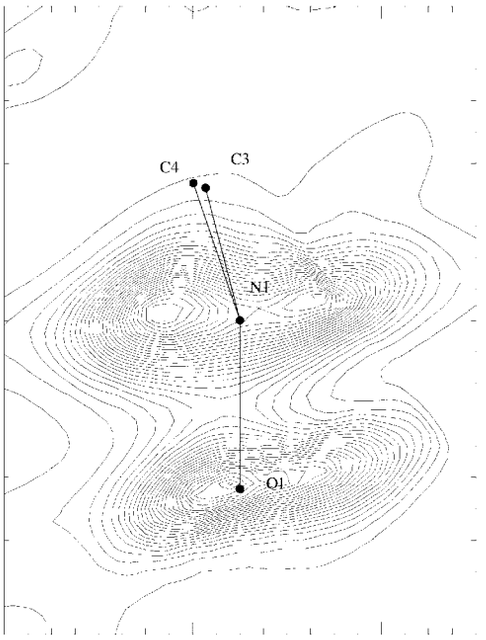

Fig. 7 Spin density reconstructed by MaxEnt and projected along the y-axis (contour step: 0.013 μ_B Å^{-2}).

Table 2 Spin populations resulting from the orbital model refinement

Atoms	Experimental results
O1	0.396 (14)
N1	0.388 (19)
C1	0.007 (11)
C2	0.006 (16)
H21	0.038 (13)
H22	−0.032 (13)
C3	−0.074 (12)
C4	0.069 (17)
C5	0.039 (17)
H51	0.017 (14)
H52	0.046 (14)
C8	0.003 (17)
H81	0.011 (12)
H82	−0.012 (12)
H83	−0.002 (15)
C9	0.012 (17)
H91	−0.029 (15)
H92	−0.001 (13)
H93	0.052 (14)
C6	−0.054 (16)
H61	0.038 (12)
H62	−0.019 (12)
H63	0.038 (13)
C7	0.021 (19)
H71	−0.014 (12)
H72	0.055 (14)
H73	0.010 (14)
N2	−0.068 (14)
C10	0.021 (18)
C11	−0.016 (17)
C12	−0.015 (16)
C13	−0.008 (13)
C14	0.041 (13)
C15	0.019 (16)
C16	0.064 (17)
Cl1	−0.058 (13)

$$\psi_M^N = -0.150(84)|2p_x\rangle + 0.184(51)|2p_y\rangle + 0.972(4)|2p_z\rangle \quad (3)$$

Fig. 10 shows a projection of the corresponding spin density along the y axis of site N1, that is onto the π plane of the NO group. The 2p orbitals, both on N1 and on O1 are neither perpendicular to N1–O1 nor to the plane C3–N1–C4. They have rotated from the z direction with an angle of 8° for N1 and 9° for O1. Considering that N1–O1 makes an angle of 163° with the plane C3–N1–C4, the 2p orbitals on N1 and O1 are practically bisecting this angle.

On the piperidine ring, the two carbon atoms which are adjacent to the aminoxyl group carry a significant spin population, but of opposed signs: −0.074(12) for C3 and +0.069(17) for C4.

On the rest of the molecule the alternation of the signs is almost perfect. The largest spin densities are carried by the amino N2 atom: −0.068(14) and the terminal chlorine atom: −0.058(13).

Theoretical spin density determination

To give a theoretical pole of comparison with the experimental results, we have performed *ab initio* calculations of the spin density of the Cl-TEMPO molecule. From previous studies on the experimental and theoretical spin densities in organic free radicals, and in particular, on the simple TEMPOL (4-hydroxy-2,2,6,6-tetramethylpiperidine-*N*-oxyl) and TEMPONE (4-oxo-2,2,6,6-tetramethylpiperidine-*N*-oxyl) molecules, parents of Cl-TEMPO,[24] it was clear that the UHF based methods[25] do not give reliable densities while the densities obtained by DFT[26] are quite close to the experimental ones. Therefore, to perform our spin density calculations, we have applied the DFT method as implemented in the program

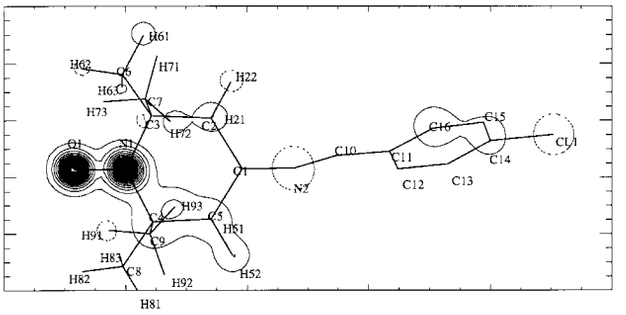

Fig. 8 Spin density reconstructed by orbital modeling and projected along the z-axis of N1: high contours (contour step: 0.05 μ_B Å^{-2}). Dashed lines represent negative spin densities.

DGAUSS.[27] At the local spin density functional level, the functional of Vosko, Wilk and Nusair[28] was utilized with the nonlocal correlational potential of Perdew[29] and the nonlocal exchange potential of Becke.[30] The DGAUSS program uses Gaussian basis sets. The different calculations were done with local density optimized basis set at the DZVP level.

The calculations were first performed for an isolated molecule and then for two interacting molecules (molecule 5 and molecule 1), in order to check the effects of the close contacts. In both cases the molecules were in their experimental low temperature crystal geometry (unpolarized neutron diffraction, $T = 4.5$ K). The atomic Mulliken spin populations of the isolated radical (first column), of the interacting molecule 5 and molecule 1 (second and third column) are displayed in Table 3, together with the experimental spin populations normalized to unity (fourth column).

Discussion

As in many other aminoxyl radicals,[31,32] most of the spin density (80% here) has been found on the NO group and a much smaller amount (20%) is delocalized on the other atoms of the molecule: on the piperidine ring, but also on the aryl part. We shall examine successively these different densities and compare them to those measured on other simple TEMPO compounds and to those calculated by the DFT method on isolated and on interacting Cl-TEMPO molecules.

i) On the NO group, the spin density has been found to be equally shared between the oxygen and the nitrogen atoms (ratio 50 : 50). In comparison, in the pure TEMPONE[32] where the molecules are quite isolated and the Curie law is followed down to a very low temperature, the ratio was found to be 47 : 53, close to the former value, favoring slightly the nitrogen site. On the other hand, in TEMPOL (4-hydroxy-2,2,6,6-tetramethylpiperidine-*N*-oxyl),[32] where the oxygen of the NO group is strongly involved in magnetic interactions through a hydrogen bond, the spin density on the oxygen atom is

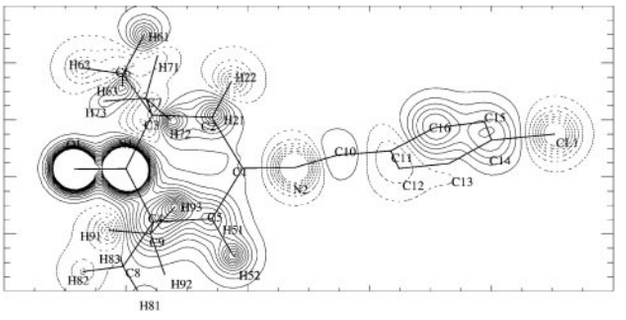

Fig. 9 Spin density reconstructed by orbital modeling and projected along the z-axis of N1: low contours. Dashed lines represent negative spin densities (contour step: 0.033 μ_B Å^{-2}).

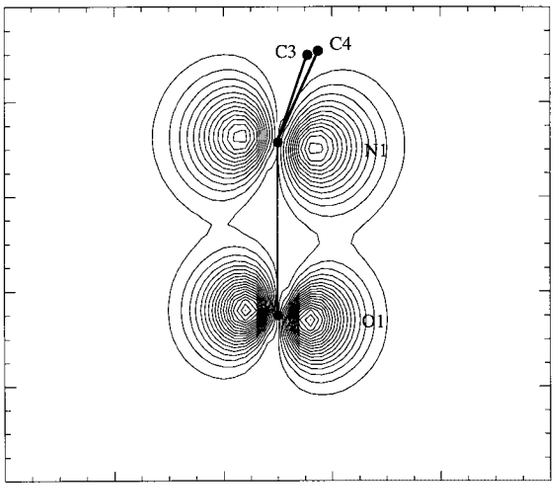

Fig. 10 Spin density on the NO group, reconstructed by orbital modeling and projected onto the π plane of the aminoxyl (contour step: 0.047 μ_B Å^{-2}).

markedly depleted and the ratio of spin populations between the oxygen and the nitrogen was reduced to 39 : 61.

Along the same line, the DFT calculations on Cl-TEMPO indicate that a larger part of the spin density is localized on the NO group (93%) and provides a ratio of 52.5 : 47.5 for the isolated molecule and 51.4 : 48.6 for the interacting molecules. We can then consider this ratio as a raw indication of the magnetic interactions passing through the oxygen of the NO radical, and the experimental ratio of 50 : 50 suggests a rather small level for these interactions.

This localized spin density has been found to correspond to a molecular wave function built from 2p orbitals of the nitrogen and the oxygen atoms. The antibonding character of this wave function has been demonstrated by the maximum entropy reconstruction of the spin density (see Fig. 7). Concerning the orientation of the 2p orbitals, we can compare it to the case of pure TEMPOL[32] as the geometry of the two molecules is quite similar with a chair conformation. In Cl-TEMPO, the bond N1–O1 makes an angle of 163° with the C3N1C4 plane. In pure TEMPOL this angle is a little flatter: 165°. In both cases, it has been found that the 2p orbitals of both nitrogen and oxygen are neither perpendicular to the N–O bond nor to the CNC plane. They are almost along the bisecting line in Cl-TEMPO (8° out of the *z* axis), they are closer to the normal to the N–O bond in pure TEMPOL (3° out of the *z* axis).

ii) On the piperidine ring, the largest spin densities, after those on oxygen and nitrogen, lie on the carbon atoms neighbouring directly the NO group. The spin populations have been found unambiguously of opposite signs: −0.075(12) on C3 and +0.070(17) on C4. This result leads us to discuss the coupling mechanism proposed by Nogami *et al.*,[5,9] to explain the interactions which exist between molecules 1, 2 and 5 inside the zig-zag sheets. This mechanism would couple, on the one hand, the N1 spin of molecule 2 with the O1 spin of molecule 1 (connection roughly parallel to ***a***) through a path N1–C4–C9–H93···O1 with an intermolecular distance of 2.49 Å between H93 and O1 (see Fig. 5a), and on the other hand the O1 spin of molecule 5 with the N1 spin of molecule 1 (connection roughly parallel to ***c***) through a path O1···H61–C6–C3–N1 with an

Table 3 Mulliken spin populations obtained with DFT calculations for the isolated radical (first column), for the interacting molecule 5 and molecule 1 (second and third column), together with the experimental spin populations normalized to unity (fourth column)

		Molecules 5 and 1 interacting		
Atoms	Isolated molecule	Molecule 5	Molecule 1	Experiment normalized to 1 μ_B
O1	0.490	0.477	0.489	0.401 (14)
N1	0.444	0.451	0.445	0.393 (19)
C1	−0.004	−0.003	−0.003	0.007 (11)
C2	0.007	0.006	0.011	0.006 (16)
H21	0.000	0.000	0.001	0.038 (13)
H22	0.000	0.000	0.000	−0.032 (13)
C3	−0.006	−0.006	−0.007	−0.075 (12)
C4	−0.008	−0.008	−0.008	0.070 (17)
C5	0.008	0.008	0.008	0.039 (17)
H51	0.000	0.000	0.000	0.017 (14)
H52	0.000	0.000	0.000	0.047 (14)
C8	0.002	0.003	0.002	0.003 (17)
H81	−0.001	−0.001	−0.001	0.011 (12)
H82	0.000	0.000	0.000	−0.012 (12)
H83	0.001	0.001	0.001	−0.002 (15)
C9	0.031	0.031	0.031	0.012 (17)
H91	−0.001	−0.001	−0.001	−0.029 (15)
H92	0.003	0.003	0.003	−0.001 (13)
H93	−0.001	−0.001	−0.001	0.053 (14)
C6	0.003	0.004	0.004	−0.055 (16)
H61	−0.001	−0.001	−0.002	0.038 (12)
H62	−0.001	−0.001	−0.001	−0.019 (12)
H63	0.001	0.001	0.001	0.038 (13)
C7	0.032	0.032	0.032	0.021 (19)
H71	0.002	0.003	0.002	−0.014 (12)
H72	−0.001	−0.001	−0.001	0.056 (14)
H73	0.000	−0.001	0.000	0.010 (14)
N2	0.000	0.000	0.000	−0.069 (14)
C10	0.000	0.000	0.000	0.021 (18)
C11	0.000	0.000	0.000	−0.016 (17)
C12	0.000	0.000	0.000	−0.015 (16)
C13	0.000	0.000	0.000	−0.008 (13)
C14	0.000	0.000	0.000	0.041 (13)
C15	0.000	0.000	0.000	0.019 (16)
C16	0.000	0.000	0.000	0.064 (17)
Cl1	0.000	0.000	0.000	−0.059 (13)

intermolecular contact distance of 2.37 Å between H61 and O1 (see Fig. 5b). The signs of the spin populations on the N, C, C, H and O atoms should alternate as a result of the hyperconjugation, with a negative sign on the hydrogen atoms. In the zig-zag sheet this should result in a ferromagnetic coupling between molecule 1 and molecule 2 as well as between molecule 1 and molecule 5. This scheme, with the proposed sign alternation is supported by the DFT calculations performed on the molecule with its actual geometry, as can be seen in Table 3. These calculations find nearly the same values −0.006 and −0.008 for the spin populations on C3 and C4. However, the experimental spin density does not show this sign alternation, and in particular, the difference of signs on C3 and C4 indicates that the coupling scheme is certainly more complex than the rather simple model which has been proposed. Let us remember that in TEMPONE, the parent compound for which, as for Cl-TEMPO, these two carbon atoms are not constrained to be identical by the symmetry elements of the space group, the spin populations were also found to be of different signs: −0.056(20) and 0.027(23).

iii) What can then be said on the coupling paths? Along the ***a*** direction, between molecule 1 and molecule 2, we can see on Table 2 that the two hydrogen atoms H72 and H93, at contact distances of 2.62 Å and 2.49 Å from atom O1 (Fig. 5a), carry rather large spin populations: 0.056(14) and 0.053(14). Even if the signs do not correspond to the proposed model, it is clear that these atoms contribute to the coupling.

Along the ***c*** direction, between molecule 1 and molecule 5, there are two methyl hydrogen atoms, bound to carbon C6, which are in contact with atom O1 and which carry a noticeable spin density: H61 at a distance 2.37 Å carries a spin population of 0.038(12) and H63, at a distance 3.40 Å (Fig. 5b) carries 0.038(13). Besides that, the methylene atom H22, bound to carbon C2, is at a distance 2.73 Å of atom O1 and has a spin population of −0.032(13). It is therefore natural to think that these hydrogen atoms and the carbons to which they are connected are implied in the magnetic interactions. Furthermore, it is possible to compare here the results of the DFT calculations performed for an isolated molecule and to molecule 5 when it is in contact with molecule 1 (see Table 3). The spin density, though underestimated for this delocalized part in the DFT calculations, is slightly (from −0.001 to −0.002 for H61) and decidedly increased (from 0.007 to 0.011 for C2) when passing from the isolated to the interacting molecule. This increase does not give the key of the magnetic interaction, but supports the proposed paths.

iv) Still along the same direction (coupling between molecule 1 and 5), the marked density found on the imino nitrogen N2 (−0.069(14)) questions whether a contact is possible with atom O1. The distance between these two atoms seems too large for a direct interaction. However, the surprising density found on the terminal chlorine atom (−0.059(13)) suggests the existence of a coupling between the N2 atom of molecule 1 and the Cl atom of molecule molecule 4, on different zig-zag sheets. The distance between these two atoms is 3.77 Å (see Fig. 4) and direct interactions are possible, weak, but enough to couple the zig-zag sheets at low temperature. There would then be an intramolecular interaction between atoms N1, N2 and Cl1 leading to a spin polarization on N2 and Cl1, followed by intermolecular interactions N2(molecule 1)–Cl1(molecule 4) and Cl1(molecule 1)–N2(molecule 4).

Conclusion

The polarized neutron investigation on the ferromagnetic aminoxyl radical Cl-TEMPO has clearly shown that 80% of the spin density is localized on the NO group of the radical, equally shared on the nitrogen and the oxygen atoms and that 20% of this density is delocalized on the other atoms of the molecule. The analysis of this delocalized part allowed to see that the scheme of the magnetic interactions between adjacent molecules is not simple but implies different paths. In particular the role of some methyl and methylene hydrogen atoms has been evidenced.

DFT calculations are in accordance with experimental results for the repartition of the spin density on nitrogen and oxygen. They nevertheless underestimate the part of the spin density which is delocalized on the rest of the molecule. They also underestimate the effects of the magnetic interactions on the spin density of adjacent molecules. However, the comparison of similar calculations for isolated and for interacting molecules is a valuable guide to discuss possible paths of the magnetic interactions.

References

1 Recent reviews on molecular magnetism: (*a*) A. Caneschi, D. Gatteschi and P. Rey, *Prog. Inorg. Chem.*, 1991, **39**, 331; (*b*) O. Kahn, *Molecular Magnetism*, VCH Publishers, Inc., New York, 1993.

2 (*a*) J. S. Miller and A. J. Epstein, *Angew. Chem., Int. Ed. Engl.*, 1994, **33**, 385; (*b*) *Magnetic properties of Organic Radicals*, ed. M. Lahti, Marcel Dekker, Inc.; New York, 1999.

3 M. Tamura, Y. Nakazawa, D. Shiomi, K. Nozawa, Y. Hosokoshi, M. Ishikawa, M. Takahashi and M. Kinoshita, *Chem. Phys. Lett.*, 1991, **186**, 401.

4 R. Chiarelli, A. Novak, A. Rassat and J. L. Tholence, *Nature (London)*, 1993, **363**, 147.

5 T. Nogami, T. Ishida, M. Yasui, F. Iwasaki, H. Iwamura, N. Takeda and M. Ishikawa, *Mol. Cryst. Liq. Cryst.*, 1996, **279**, 97.

6 (*a*) K. Togashi, R. Imachi, K. Tomioka, H. Tsuboi, T. Ishida, T. Nogami, N. Takeda and M. Ishikawa, *Bull. Chem. Soc. Jpn.*, 1996, **69**, 2821; (*b*) T. Nogami and T. Ishida, *Mol. Cryst. Liq. Cryst.*, 1997, **296**, 305; (*c*) T. Nogami, R. Imachi, T. Ishida, N. Takeda and M. Ishikawa, *Mol. Cryst. Liq. Cryst.*, 1997, **305**, 211.

7 Yu. S. Karimov, *Sov. Phys. JETP (Engl. Transl.)*, 1970, **30**, 1062.

8 F. Iwasaki, J. H. Yoshikawa, H. Yamamoto, E. Kan-nari, K. Takada, M. Yasui, T. Ishida and T. Nogami, *Acta Crystallogr. Sect. B*, 1999, **255**, 231.

9 T. Nogami, T. Ishida, M. Yasui, F. Iwasaki, N. Takeda, M. Ishikawa, T. Kawakami and K. Yamaguchi, *Bull. Chem. Soc. Jpn.*, 1996, **69**, 1841.

10 (*a*) T. Kawakami, A. Oda, S. Takeda, W. Mori, T. Ishida, M. Yasui, F. Iwasaki, T. Nogami and K. Yamaguchi, *Mol. Cryst. Liq. Cryst.*, 1997, **306**, 141; (*b*) G. Maruta, S. Takeda, T. Kawakami, W. Mori, R. Imachi, T. Ishida, T. Nogami and K. Yamaguchi, *Mol. Cryst. Liq. Cryst.*, 1997, **306**, 307.

11 G. Maruta, S. Takeda, R. Imachi, T. Ishida, T. Nogami and K. Yamaguchi, *J. Am. Chem. Soc.*, 1999, **121**, 424.

12 R. Imachi, T. Ishida, T. Nogami, S. Ohira, K. Nishiyama and K. Nagamine, *Chem. Lett.*, 1977, 233.

13 E. Ressouche, J. X. Boucherle, B. Gillon, P. Rey and J. Schweizer, *J. Am. Chem. Soc.*, 1993, **115**, 3610; M. A. Aebersold, B. Gillon, O. Plantevin, L. Pardi, O. Kahn, P. Bergerat, I. von Seggern, F. Tuczek, L. Ohrstrom, A. Grand and E. Lelievre-Berna, *J. Am. Chem. Soc.*, 1998, **120**, 5238.

14 Y. Pontillon, T. Akita, A. Grand, K. Kobayashi, E. Lelievre-Berna, J. Pecaut, E. Ressouche and J. Schweizer, *J. Am. Chem. Soc.*, 1999, **121**, 10126; Y. Pontillon, A. Caneschi, D. Gateschi, A. Grand, E. Ressouche, R. Sessoli and J. Schweizer, *Chem. Eur. J.*, 1999, **5**(12), 3616; Y. Pontillon, E. Lelievre-Berna, A. Caneschi, D. Gatteschi, R. Sessoli, E. Ressouche and J. Schweizer, *J. Am. Chem. Soc*, 1999, **121**, 5342.

15 Among the 1944 reflections measured on the first crystal, 1209 were independent and among the 1135 reflections measured on the second crystal, 897 were independent. The maximum values of $\sin\theta/\lambda$ were 0.65 $Å^{-1}$ for crystal **1** and 0.74 $Å^{-1}$ for crystal **2**.

16 W. R. Busing, K. O. Martin and H. A. Levy, ORNL Report 59-37, Oak Ridge National Laboratory: Oak Ridge, TN, 1991.

17 $I = F^2 G(I_0)$ with $G(I_0) = 1/\sqrt{\{1 + [(2gL\lambda^3)/(V^3 \sin 2\theta)]F_N^2\}}$ where I_0 is the 'kinematics' intensity, V is the unit cell volume and L the mean crystal traversing path. L, λ, V and F^2 are expressed in cm, Å, $Å^3$ and 10^{-12} cm^2 respectively. g is a dimensionless number, characteristic of the mosaicity of each crystal (the refinement

yielded $g = 135(3)$ for the first crystal and 38 (3) for the second crystal).
18 The expression for the flipping ratio was modified to include corrections due to the imperfection of the beam, the extinction and the nuclear polarization of the hydrogen atoms. The nuclear structure factors were calculated from the low temperature crystal structure.
19 E. Ressouche and J. Schweizer, *J. Neutron Res.*, 1996, **4**, 15.
20 R. J. Papoular and B. Gillon, *Europhys. Lett.*, 1990, **13**, 429.
21 B. Gillon and J. Schweizer, in *Molecules in Physics, Chemistry and Biology*, vol II, ed. J. Maruani, Kluwer, Dordrecht, 1989, pp. 111–147.
22 A. Zheludev, V. Barone, M. Bonnet, B. Delley, A. Grand, E. Ressouche, P. Rey, R. Subra and J. Schweizer, *J. Am. Chem. Soc.*, 1994, **116**, 2019.
23 N. J. Hehre, R. F. Stewart and J. A. Pople, *J. Chem. Phys.*, 1969, **51**, 2657.
24 E. Ressouche, Doctoral thesis, University J. Fourier, 1991.
25 C. Moller and M. S. Plesset, *Phys. Rev.*, 1934, **46**, 618; I. Shavitt, "Methods of Configurational Interaction", in *Modern Theoretical Chemistry*, vol. 3, ed. H. F. Shaefer, III, Plenum Press, New York, 1977, p. 189.
26 W. Kohn and L. J. Sham, *Phys. Rev. A*, 1965, **1133**, 140.
27 DGAUSS UniChem4, Cray Research Inc., Cray Research Park, 655 Lone Oak Drive, Eagan, MN 55121.
28 S. H. Vosko, L. Wilk and M. Nausair, *Can. J. Phys.*, 1980, **58**, 1200.
29 J. P. Perdew, *Phys. Rev. B*, 1986, **33**, 8822.
30 A. D. Becke, *Phys. Rev. A*, 1988, **38**, 3098.
31 P. J. Brown, A. Capiomont, B. Gillon and J. Schweizer, *Mol. Phys.*, 1983, **48**, 753.
32 D. Bordeaux, J. X. Boucherle, B. Delley, B. Gillon, E. Ressouche and J. Schweizer, *Z. Naturforsch., Teil A*, 1993, **48**, 117.